GPD and TDA measurements based on hard exclusive pion electroproduction with CLAS at JLAB

S. Diehl[1,2], K. Joo[2] for the CLAS collaboration

[1]2nd Physics Institute, Justus Liebig University Giessen, 35410 Giessen, Germany
[2]Department of Physics, University of Connecticut, Storrs, CT 06269, USA
E-mail: stefan.diehl@exp2.physik.uni-giessen.de

Besides a GPD based description, the collinear factorisation theorem of QCD also allows a TDA based description of the hard exclusive pion electroproduction. Both descriptions provide access to different kinematic regions and therefore give us insights into different aspects of the 3 dimensional nucleon structure. To understand the complete reaction mechanism and the validity of the different models, experimental studies over the full kinematic range have to be performed. In this work measurements of the beam-spin asymmetry have been performed over a wide range of kinematics in the deep inelastic regime for the hard exclusive e p → e n π^+ reaction using the CEBAF Large Acceptance Spectrometer (CLAS) and a 5.5 GeV polarized electron beam at Jefferson Lab (JLAB). The ϕ dependence of the BSA as well as the Q^2, x_B and t dependence of the extracted moments will be presented. A clear sign change of the BSA can be observed between pions emitted in forward and backward direction with a smooth transition around 90° in CM.

Keywords: pion electroproduction; beam spin asymmetry; GPD; TDA; CLAS.

1. Introduction

Studying exclusive pion electroproduction can provide valuable insights into the 3 dimensional structure of the nucleon, since the size of the probe as well as the photon virtuality Q^2 and the momentum transfer to the nucleon t can be varied simultaneously. On the theoretical side, the colinear factorization theorem allows different descriptions of the hard exclusive pion production for different kinematic regimes.

A first description of the process is given by generalized parton distributions (GPD). GPDs are universal structure functions, which describe the hadronic structural information in terms of quark-gluon degrees of freedom [1-2]. They are a good tool to investigate the nature and the origin of the nucleon spin. In the impact parameter space, they can be interpreted as spatial femto-photographs of the nucleon structure in the transverse plane. To ensure factorization, the GPD based description requires large Q^2 and s values and a small t channel contribution. Experimentally this corresponds to a pion going in forward direction.

Besides the GPD based description the collinear factorization theorem also allows a description of the hard exclusive processes by Transition Distribution Amplitudes (TDAs) [3-6]. TDAs are universal structure functions which encode a physical picture, which is very similar to that of GPDs. They probe the partonic correlation between states of different baryonic charge and therefore give us access to non-minimal Fock components of the baryon light cone wave function. The TDA formalism is valid for large Q^2 and s and for a small u channel transfer, which correspond to large -t values and is therefore complementary to the GPD kinematic regime. Graphically this means that the proton takes most of the momentum of the virtual photon and is emitted in the forward direction, while the a pion from the mesonic cloud of the nucleon is emitted with low momenta in the backward direction. Therefore the process can be used to probe the structure of the mesonic cloud inside the nucleon.

A comparison between the GPD and the TDA mechanism for the exclusive pion production is given in Fig. 1.

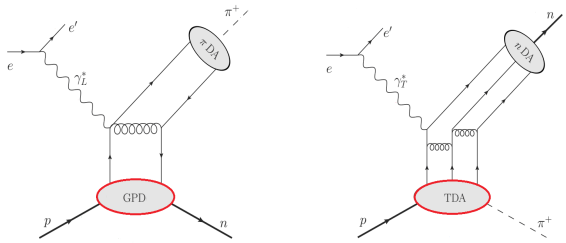

Fig. 1. Schematic diagram for the exclusive e p → e n π^+ reaction for a GPD based description (left) and for a TDA based description (right).

The cross section of the hard exclusive pion production in terms of transverse, longitudinal, transverse-transverse and longitudinal-transverse interference structure functions (T, L, TT, TL, and TL´) is given by:

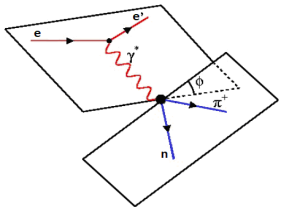

$$\frac{d\sigma}{d\Omega_{e'}d\epsilon_{e'}\Omega_\pi} = \Gamma\frac{d\sigma_\nu}{d\Omega_\pi} \qquad \Gamma = \frac{\alpha_{em}}{2\pi^2}\frac{E_{e'}}{E_0}\frac{W^2}{Q^2}\frac{1}{1-\epsilon}$$

$$\frac{d\sigma_\nu}{d\Omega_\pi} = \frac{d\sigma_T}{d\Omega_\pi} + \epsilon_L\frac{d\sigma_L}{d\Omega_\pi} + \sqrt{2\epsilon_L(1+\epsilon)}\frac{d\sigma_{TL}}{d\Omega_\pi}\cos(\phi)$$
$$+\epsilon\frac{d\sigma_{TT}}{d\Omega_\pi}\cos(2\phi) + h\sqrt{2\epsilon_L(1-\epsilon)}\frac{d\sigma_{TL'}}{d\Omega_\pi}\sin(\phi)$$

It depends on the virtuality Q^2 and the transverse and longitudinal polarizations of the virtual photon (ε, ε_L) as well as on Bjorken x_B, the squared momentum transfer t to the proton, the angle ϕ between the leptonic and the hadronic planes and the beam polarization h. Measurements of the cross section in backward kinematics have been performed within the CLAS collaboration in Ref. [7] and show a good agreement with the $1/Q^8$ scaling behavior expected from the TDA mechanism. By substituting the terms in front of the ϕ dependences with the moments $A_{UU}^{\cos(\phi)}$, $A_{UU}^{\cos(2\phi)}$ and $A_{LU}^{\sin(\phi)}$ and introducing the unpolarized

cross section $d\sigma_0$, the cross section can be simplified to:

$$d\sigma = d\sigma_0 \cdot (1 + h \cdot A_{LU}^{\sin(\phi)} \sin(\phi) + A_{UU}^{\cos(\phi)} \cos(\phi) + A_{UU}^{\cos(2\phi)} \cos(2\phi)) \quad (1)$$

Based on the three moments, the beam-spin asymmetry can be defined as:

$$BSA = \frac{\sigma^+ - \sigma^-}{\sigma^+ + \sigma^-} = \frac{A_{LU}^{\sin(\phi)} \sin(\phi)}{1 + A_{UU}^{\cos(\phi)} \cos(\phi) + A_{UU}^{\cos(2\phi)} \cos(2\phi)} \quad (2)$$

where σ± is the cross section for the two helicity states with the spin parallel (+) and anti-parallel (-) to the beam direction.

2. Experimental setup and particle identification

The analyzed data was recorded with the CEBAF Large Acceptance Spectrometer (CLAS) in hall B at Jefferson LAB in 2003, using a 5.5 GeV longitudinally polarized electron beam, interacting with an unpolarized hydrogen target. The average beam polarization was 74.9 ± 2.4(stat) %. The CLAS detector is build around a torus magnet, which divides the setup in six sectors. Each sector contains 3 regions of drift-chambers to determine the momentum of charged particles within the torus field, a Cherenkov counter and a time of flight system for the identification of charged particles and an electromagnetic calorimeter to identify electrons and to detect photons.

3. Analysis procedure

As a first step, the deep inelastic scattering region was selected with cuts on $Q^2 > 1$ GeV² and $W > 2$ GeV. To separate the forward and backward kinematic region, cuts on the Mandelstam variables t and u, and on the polar angle θ_{CM} of the π^+ in the centre of mass frame were applied. The forward direction is defined as $-t < 1.5$ GeV² and $\cos(\theta_{CM}) > 0$ and for the backward direction, cuts on $-u < 2.0$ GeV² and $\cos(\theta_{CM}) < 0$ are used.

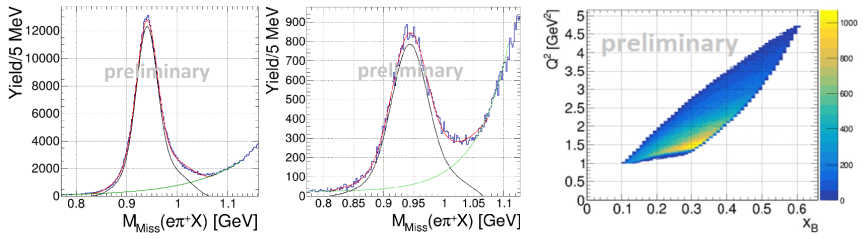

Fig. 3. Missing mass of $e\pi^+X$ in the forward region (left) and in the backward region (central). The black line shows the signal and the green line the fitted background contribution. The right plot shows the kinematic coverage of the exclusive $ep \rightarrow en\pi^+$ events in Q^2 and x_B.

Since for the reaction ep → enπ^+ only electrons and pions can be detected by CLAS, the exclusive events are selected by a cut on the missing neutron mass. The fitted missing neutron peak and its background are shown in Fig. 3 (left and central) for the forward and backward region. The fit has been performed for each kinematic bin to determine the signal to background ratio. Fig. 3 (right) shows the kinematic coverage of the exclusive events in Q^2 and x_B.

4. Results

Experimentally, the beam spin asymmetry can be calculated as $(1/P_e)\cdot(N_i^+-N_i^-)/(N_i^++N_i^-)$ with the average beam polarization P_e and the count rates $N^\pm$ in a specific bin with positive and negative helicity. The beam-spin asymmetry as a function of ϕ for the forward and backward kinematic region, integrated over the other kinematic variables (Q^2 and x_B) is shown in Fig. 4.

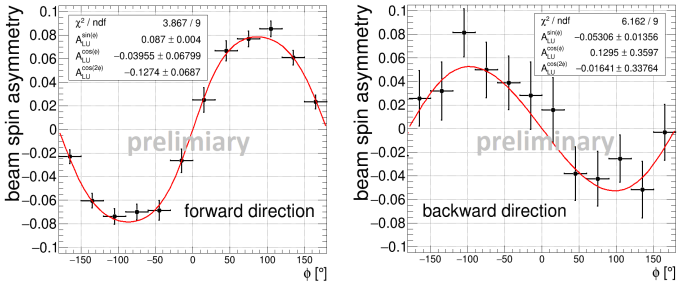

Fig. 4. Beam spin asymmetry in forward (left) and backward direction (right). Both plots are integrated over all Q^2 and x_B bins. The shown result is preliminary.

The ϕ dependence is fitted with Eq. 2. A clear sign change of $A_{LU}^{\sin(\phi)}$ can be observed between the forward and backward kinematic region. To investigate the transition between the forward and backward kinematics more closely, $A_{LU}^{\sin(\phi)}$ has been extracted for different bins in -t, Q^2 and x_B. Based on the signal to background ratio from the fit of the missing mass and based on the asymmetry of the background determined from a missing mass interval on the right side of the missing neutron peak in Fig. 3, a background subtraction has been performed in each bin.

For the systematic uncertainty, thirteen different sources were considered, including the particle identification, the beam polarization and the influence of the higher order moments. A fast MC simulation was used to determine the impact of acceptance effects, which was found to be negligible. Each source of systematic uncertainty stays well below the statistical uncertainty. The total systematic uncertainty is defined as the square root of the quadratic sum of all contributions. Fig. 5 shows the -t dependence of $A_{LU}^{\sin(\phi)}$ including the statistical and systematic uncertainty.

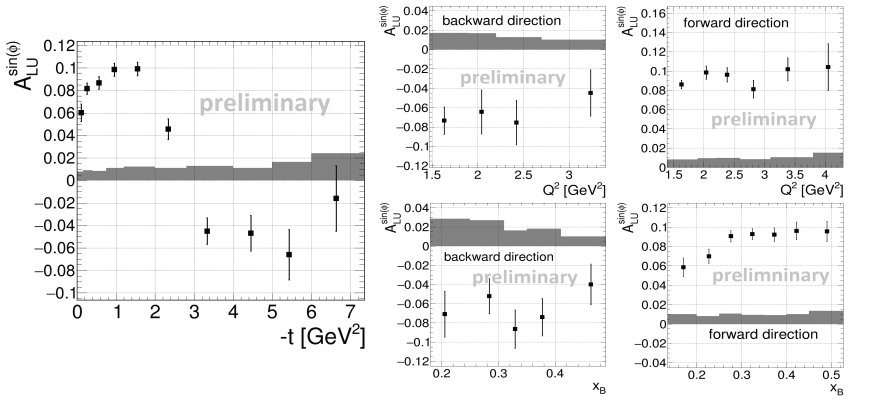

Fig. 5. Dependence of $A_{LU}^{\sin(\phi)}$ on -t (left), Q^2 (upper right) and x_B (lower right) [preliminary]. The data points show the statistical uncertainty, while the shaded area represents the systematic.

A clear transition from positive values up to a magnitude of 0.10 in the forward kinematic region (small -t) to negative values up to a magnitude of -0.06 in the backward kinematic region (large -t) can be observed. As expected the magnitude of $A_{LU}^{\sin(\phi)}$ decreases for very small and large -t values. The smooth transition happens around -t = 3 GeV², which corresponds to a θ_{CM} of 90°. Also the Q^2 and x_B dependence of $A_{LU}^{\sin(\phi)}$ in Fig. 5 clearly show, that $A_{LU}^{\sin(\phi)}$ is negative for all Q^2 and x_B bins in backward direction, while it is positive for all bins in forward direction. Since the forward kinematic region can be described by GPDs, while the backward kinematic region is described by TDAs, this sign change may indicate the transition between the GPD and TDA based formalisms.

Acknowledgments

The authors acknowledge very helpful discussions with B. Pire, K. Semenov-Tian-Shansky and P. Kroll as well as the outstanding efforts of the staff of the Accelerator and the Physics Divisions at JLAB in making this experiment possible. The work is partly supported by DOE grant no: DE-FG02-04ER41309.

References

[1] D. Mueller et al., Fortsch. Phys. 42, 101 (1994).
[2] X. Ji, Phys. Rev. Lett. 78, 610 (1997).
[3] L.L. Frankfurt et al., Phys. Rev. D 60, 014010 (1999).
[4] B. Pire and L. Szymanowski, Phys. Lett. B 622, 83 (2005).
[5] B. Pire and L. Szymanowski, Phys. Rev. D 71, 111501 (2005).
[6] J. P. Lansberg, B. Pire, L. Szymanowski, Phys. Rev. D 75, 074004 (2007).
[7] K. Park et al., CLAS Collaboration, Phys. Lett. B 780 340345, (2018).